RAD Conference Proceedings, vol. 7, pp. 1-5, 2023
ISSN 2466-4626 (online) | DOI: 10.21175/RadProc.2023.01
www.rad-proceedings.org

PHOTOACTIVATION STUDY OF ^{163}TB β-DECAY

Anastasiia Chekhovska*[1], David Chvátil[2], Tamara Krasta[1], Ivana Krausova[2], Vaclav Olšanský[2], Daina Riekstiņa[1]

[1]Institute of Solid State Physics of the University of Latvia
[2]Nuclear Physics Institute of the Czech Academy of Sciences

***Abstract**. The enriched ^{164}Dy and natural dysprosium targets were activated with the bremsstrahlung beam at end-point energies 7.17, 8.11, 9,75, 12.12, 13.75, 16.6, 18.34, 20.36, and 22.82 MeV. The decay γ-spectra measured with HPGe detector up to 2.4 MeV energy were used to determine yields of the photoactivation reaction ^{164}Dy(γ,p)^{163}Tb. The γ-spectra following the ^{164}Dy photoactivation reaction with 20.36 MeV photons allowed to develop the level scheme of ^{163}Dy including 37 levels up to 1.44 MeV excitation energy. A number of ^{163}Dy levels and γ-lines were observed in the β-decay of ^{163}Tb for the first time. The proposed level scheme of ^{163}Dy was compared with the results of quasiparticle-plus-rotor interaction model calculations.*

***Keywords**: Enriched ^{164}Dy and ^{nat}Dy targets, bremsstrahlung E=20.36 MeV, HPGe detector, ^{164}Dy(γ,p)^{163}Tb reaction yield, ^{163}Tb β-decay, ^{163}Dy level scheme, quasiparticle-plus-rotor model calculations.*

1. INTRODUCTION

Problems related with the cosmic nucleosynthesis of elements heavier than iron are presently one of the most discussed fundamental astrophysics topics. Photonuclear reactions are an essential component of these processes (see, e.g., [1]). Detailed knowledge about photonuclear reaction cross-sections, γ-ray strength functions and level densities is important for the study of element abundances in the Universe.

Lanthanides, such as gadolinium, terbium, dysprosium, are widely used as dopants in different convertors for radiation detecting and radiography. The photonuclear reaction cross-section data are important for prediction of properties and behavior of different materials subjected to high energy and fluence radiation.

Deformed and transitional nuclei of the 150<A<190 region are an important testing ground for nuclear structure models and the study of NN-interaction potential. Hence, knowledge of structure and reaction properties of these nuclei is very important for fundamental nuclear theory development.

The advantage of photonuclear reactions is the absence of Coulomb barrier in the entrance channel. However, earlier photonuclear reaction studies were hindered by a limited access to intense photon beams. Nowadays, powerful γ-sources produced by modern accelerators and lasers in combination with high-precision detectors allow to obtain new more detailed experimental information both about nuclear structure and nuclear interactions.

The β-decay of ^{163}Tb nuclei ($T_{1/2}$=19.5 min) in the bremsstrahlung photoactivation reaction ^{164}Dy(γ,p)^{163}Tb was studied in 1966 [2]. In 1971, a more detailed study [3] has been published in which the ^{163}Dy(n,p)^{163}Tb reaction was used for production of ^{163}Tb nuclei. Both papers included results of single β- and γ-spectra measurements, as well as βγ and γγ coincidence measurements. On their basis, the level scheme of ^{163}Dy has been proposed and interpreted in terms of rotational bands based on Nilsson single-particle states. These experimental data about β-decay of ^{163}Tb are presently adopted in the international nuclear data bases [4]. Available experimental information about photonuclear reaction cross-sections for dysprosium isotopes is limited, and there is no reported data about ^{164}Dy(γ,p)^{163}Tb reaction.

The aim of present study is to obtain new precise information about yields of photoactivation reactions ^{164}Dy(γ,p)^{163}Tb and levels of ^{163}Dy excited in the β-decay of ^{163}Tb. The photoactivation experiment is performed using the bremsstrahlung photons. Similar experiments have been published recently for ^{nat}Ni [5] and ^{nat}Gd [6] targets.

2. EXPERIMENTAL

Two targets were prepared: one made of 0.198(2) mg Dy_2O_3 enriched to 97.8% of ^{164}Dy, and another of 0.368(1) mg natural Dy. Both targets were activated using the bremsstrahlung photons with the end-point energies $E_{\gamma max}$ = 7.17, 8.11, 9.75, 12.12, 13.79, 16.6, 18.34, 20.36, and 22.82 MeV at the microtron MT-25 of the Nuclear Physics Institute of the Czech Academy of Sciences (Prague). Scheme of the experimental set-up is shown on Figure 1.

* E-mail of the corresponding author – anastasiia.chekhovska@cfi.lu.lv

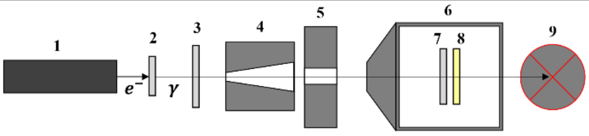

Figure 1. Experimental set-up.

[1]Microtron, [2]Convertor (with two W targets 1.5 and 3 mm and one Sn foil 0.2 mm), [3]Target with combined Al-Cu scattering foils, [4]Primary conical stainless steel collimator, [5]Secondary square W-steel collimator, [6]Water-cooled chamber, [7]Research target, [8]Monitor target (Cu or Au), [9]Absorber.

The irradiation times were chosen with regard to specific target decay characteristics. At 7.17, 8.11, 9.75, 12.12, and 13.79 MeV end-point energies, the targets were irradiated for 20 min; at 16.6, 18.34, and 20.36 MeV energies – for 15 min; and at 22.82 MeV – for 10 min. The cooling time (t_{cool}) for irradiated sample was chosen to be as short as possible for subsequent γ-spectra measurements in the low-background room.

The decay γ-spectra were measured in the energy range from 0 to 2400 keV with a high resolution HPGe detector with the 78% efficiency and energy resolution of FWHM 1.8 keV for 1332 keV γ-line of ^{60}Co. The background γ-spectrum was registered as well in order to facilitate isotopic assignment of registered γ-lines. Measurement times varied with the collected statistics. The evaluated half-widths of ^{163}Dy lines were in the range from ~0.6 keV up to ~2 keV in dependence from energy and relative intensity.

The spectrum obtained after irradiation of the enriched ^{164}Dy target with 20.36 MeV bremsstrahlung was used for the study of ^{163}Tb β-decay following the ^{164}Dy(γ,p)^{163}Tb reaction. In order to confirm the isotopic assignment of ^{163}Dy γ-lines, their intensities were compared in the spectra obtained from the enriched ^{164}Dy and natural Dy targets as well as in the spectra following the irradiation with 22.82 MeV photons and measured after longer cooling times (~9 min and ~ 1 h).

Table 1 presents irradiation, cooling and measurement times for enriched and natural dysprosium targets in the case of 20.36 and 22.82 MeV bremsstrahlung photons. In addition, the absorbed dose values for irradiated samples are given.

Table 1. Time schedules of the experiments with 20.36 MeV and 22.82 MeV bremsstrahlung photons.

t_{irr} [min]	t_{cool} [s]	t_{meas} [s]	D [kGy]
^{164}Dy; $E_{\gamma max}$ =20.36 MeV			
15	195	618.93	14.48
^{nat}Dy; $E_{\gamma max}$ =20.36 MeV			
15	171	720.70	14.43
^{164}Dy; $E_{\gamma max}$ =22.82 MeV			
10	547	601.16	11.78
^{nat}Dy; $E_{\gamma max}$ =22.82 MeV			
10	201	400.63	11.78

Figure 2 shows portions of measured γ-ray spectra from enriched ^{164}Dy and ^{nat}Dy targets.

3. Results

The energies and intensities of γ-rays following the β-decay of ^{163}Tb nuclei (Q(β)=1.785(4) MeV) were used for the development of ^{163}Dy level scheme. Obtained level scheme (Figs. 3 and 4) includes 37 levels up to 1.44 MeV energy, mostly with spin values 1/2, 3/2, 5/2, and 7/2, populated via β-decay of the ^{163}Tb 3/2$^+$[411] ground-state. Two low-lying 9/2$^-$ and 11/2$^-$ levels are populated via γ-transitions from higher lying ^{163}Dy states. The total number of γ-transitions placed in the level scheme of ^{163}Dy is 133. Eleven γ-transitions assigned to ^{163}Dy remained unplaced.

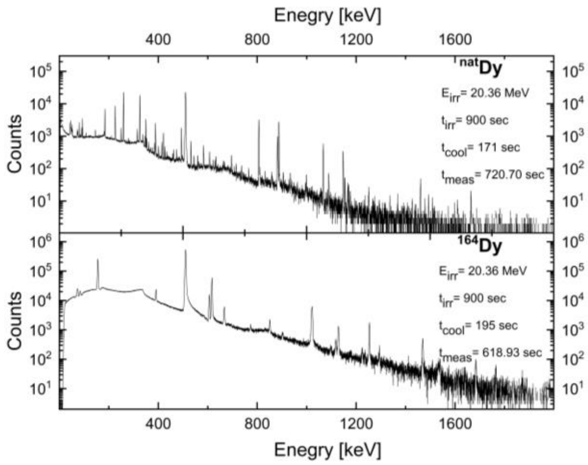

Figure 2. Decay γ-ray spectra after activation of the ^{nat}Dy and ^{164}Dy targets with 20.36 MeV bremsstrahlung.

The previously known ^{163}Dy level scheme from β-decay of ^{163}Tb [2,3] has been extended by 13 levels and 44 γ-transitions. In Figs. 3 and 4, the newly included γ-transitions are marked by crosses (13 new transitions are proposed, and 31 transitions were not observed earlier in β-decay). The energy values of earlier known levels [4] whose population in β-decay is registered for the first time are underlined.

The level energies of ^{163}Dy were obtained via a least squares fit procedure using (when available) the more precise γ-transition energy values from the (n,γ) reaction measurements [4].

4. DISCUSSION

Structure of 150<A<190 region deformed odd nuclei is interpreted in the frameworks of the quasiparticle plus rotor interaction model (QRM). Excited levels below ~ 3 MeV energy are classified in terms of rotational bands based on Nilsson quasiparticle states Ωπ[NnzΛ] in the mean field potential of the deformed even-even core.

The Kπ=5/2- ground state of 163Dy belongs to the 5/2-[523] Nilsson orbit which is closest to the Fermi level in the case of N=97 neutrons. Figure 5 presents the systematics of experimentally observed bandhead level energies and their structure assignments for N=95, 97 and 99 isotopes of gadolinium, dysprosium, and erbium neighboring to 163Dy. Data are taken from the ENSDF data base. Green color lines depict quasiparticle-vibrational states proposed earlier by other authors.

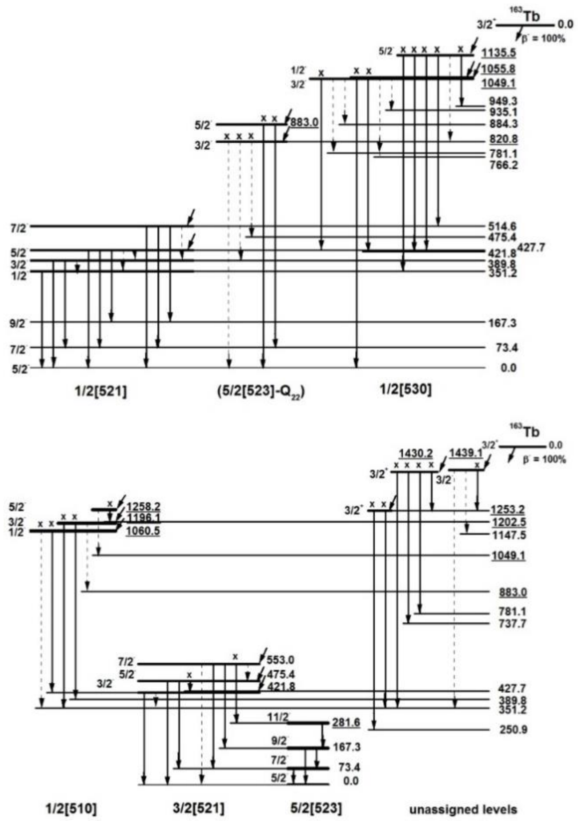

Figure 3. Negative parity levels of ^{163}Dy populated in the β-decay of ^{163}Tb.

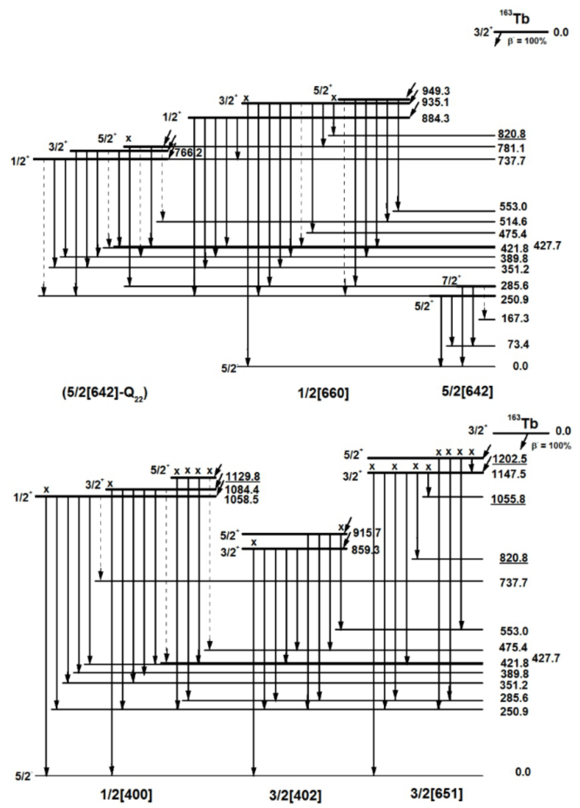

Figure 4. Positive parity levels of ^{163}Dy populated in the β-decay of ^{163}Tb.

The structure of odd neutron nuclei around N=97 is characterized by a high number of K=1/2 rotational bands below 2 MeV. Also, the two lowest quasiparticle states 5/2-[523] and 5/2+[642] belong to high j value orbitals h9/2 and i13/2. All these factors result in a very strong mixing and odd-even spin value level splittings observed not just in K=1/2 bands, but in K=3/2 bands as well.

In order to confirm structure interpretation of the developed 163Dy level scheme (Figures 3 and 4), we have performed QRM calculations employing the modified oscillator program package described in [7]. The axially-symmetric core deformation parameters where chosen according to trends outlined in [8] as ε2=0.255, and ε4=-0.02. For the rest of mean field potential parameter the standard [7] values were used: κ4=0.07; μ4=0.39; κ5=0.062; μ5=0.43; κ6=0.062; μ6=0.34, and the pairing strength G·A=g0-g1·(N-Z)/A, where g0=19.2 MeV, and g1=7.4 MeV. The core moment of inertia parameter value A1=13.53 keV has been evaluated from the 81 keV energy of the first 2+ level in 162Dy.

The QRM calculated bandhead energies of lowest quasiparticle states in ^{163}Dy are shown in Figure 5 with red lines. One can see that the general agreement between experimental and calculated bandheads is satisfactory. However, the model predicted level density is lower than the experimentally observed. Obviously, due to strong mixing and increased role of spin-orbital interaction in the case of low-lying $h_{9/2}$, $h_{11/2}$ and $i_{13/2}$ orbitals, the standard values of the single-particle potential parameters κ and μ, as well as the moment of inertia parameter should be adjusted.

Systematics of quasiparticle states in neighbouring nuclei ^{159}Gd, ^{161}Dy and ^{165}Er (Fig. 5) shows a presence of the low-lying $i_{13/2}$ hole state $1/2^+[660]$ which is confirmed by our QRM calculations as well. We propose to that role the $K^\pi=1/2^+$ rotational band at 884.3 keV basing on the decay pattern of band levels mostly via intense E1 transitions to the levels of the $1/2^-[521]$ band at 351.2 keV. In [4], the 884.3 keV band is interpreted as the $5/2^-[523]$ octupole vibration band with a large component of the $1/2^+[660]$ state. Since the bandhead systematics do not indicate a presence of octupole vibrations in neighbouring odd nuclei, we believe that the assignment of the $1/2^+[660]$ configuration to the 884.3 keV band is more convincing.

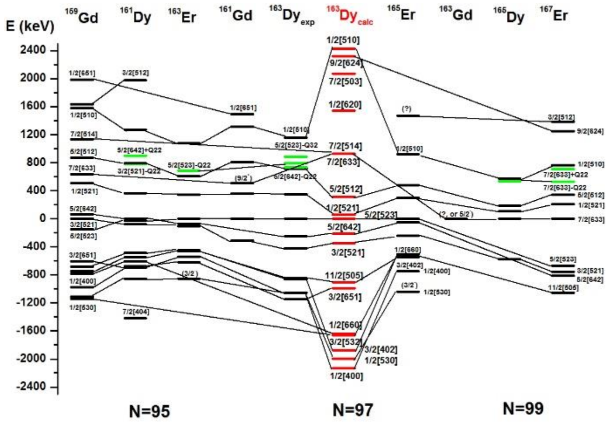

Figure 5. Systematics of ENSDF adopted odd neutron states in Gd, Dy and Er nuclei with N=95÷99 and comparison with the values obtained for ^{163}Dy in our QRM calculations.

Measured γ-intensities from spectra obtained in the bremsstrahlung energy range from 8.11 MeV to 22.82 MeV were used to determine experimental yields of ^{164}Dy(γ,p)^{163}Tb reaction which were compared with theoretical predictions using the statistical nuclear reaction theory code TALYS [9].

The experimental activation yield $Y(E_{\gamma\ max})$ of the ^{164}Dy(γ,p)^{163}Tb-reaction normalized to unit bremsstrahlung flux $\phi(E_j)$ was determined from the measured intensities S_γ of several strong γ-transitions (177.4, 212.2, 250.8, 316.4, 338.5, 351.2, 389.8, 421.9, 494.5, 507.5, 533.0, 583.9 and 633.4 keV) following the β-decay of ^{163}Tb to ^{163}Dy. The yield values were evaluated using the simple activation equation:

$$\frac{S_\gamma \cdot \lambda}{n \cdot \varepsilon \cdot I_\gamma \cdot \phi(E_j)} = Y(E_{\gamma\max}) \cdot \left(1 - e^{-\lambda t_{irr}}\right) \cdot e^{-\lambda t_{cool}} \cdot \left(1 - e^{-\lambda t_{meas}}\right) \quad (1)$$

in which λ is the radioactive decay constant, n is the number of nuclei in the irradiated target, ε is the full energy peak detection efficiency, I_γ is decay intensity value per one decay.

Our experimental values of the integral yields for ^{164}Dy(γ,p)^{163}Tb reaction on ^{164}Dy and ^{nat}Dy targets are presented in Fig.6 by the red and dark circles, respectively. Colored curves show the results of theoretical calculations based on the statistical theory of nuclear reactions with different variations of the optical potential parameters for nuclear level density and γ-ray strength function.

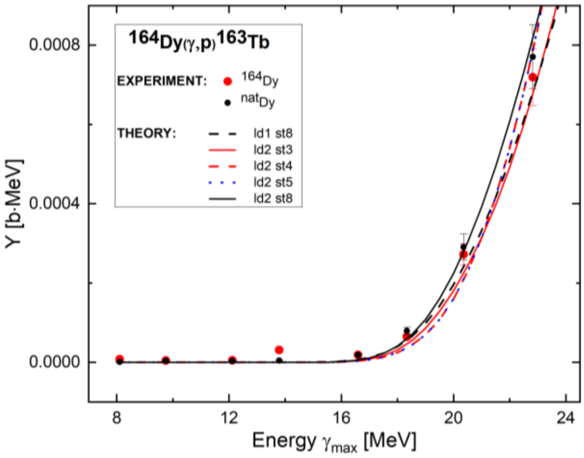

Figure 6. Experimental and theoretical yields of ^{164}Dy(γ,p)^{163}Tb reaction.

The theoretical calculations were performed using the TALYS 1.95 version. In Fig.6, following notations are used: ld1 denotes a constant temperature Fermi gas model [10], and ld2 – a back-shifted Fermi gas model [11] for the nuclear level density; while st3, st4, st5 and st8 denote the Hartree-Fock BCS model [12], Hartree-Fock-Bogolyubov model [13], Goriely's hybrid model [14] and Gogny D1M HFB+QRPA model [15] for the γ-ray strength function, respectively. (The presented statistical model variants are those which give the best correspondence with our experimental results).

From Figure 6 one can see that the best agreement with observed experimental ^{164}Dy(γ,p)^{163}Tb yield is obtained in the case of statistical theory with phenomenological optical potential using the back-shifted Fermi gas model level density and Gogny radiation strength function parameters.

The observed difference of experimental ^{164}Dy(γ,p)^{163}Tb yields in the case of enriched ^{164}Dy and ^{nat}Dy targets can be explained by unseparated intensity admixtures from the close lying γ-lines following the decay of other dysprosium isotope reaction products.

5. Conclusions

1. The decay γ-spectra of ^{163}Tb were obtained via photoactivation reaction ^{164}Dy(γ,p)^{163}Tb using the microtron bremsstrahlung photons in the energy range from 7.17 to 22.82 MeV.

2. The evaluation of γ-spectra following β-decay of ^{163}Tb allowed to develop the level scheme of ^{163}Dy including 37 levels up to 1.44 MeV energy. The earlier established ^{163}Tb decay scheme has been extended with 13 levels and 44 newly placed γ-transitions of ^{163}Dy.

3. The results of performed quasiparticle-plus-rotor model calculations show satisfactory agreement with the earlier proposed structure interpretation of ^{163}Dy rotational bands. The 1/2$^+$[660] quasiparticle state is assigned to the K^π=1/2$^+$ rotational band at 884.3 keV.

4. Comparison of the obtained experimental yields of ^{164}Dy(γ,p)^{163}Tb reaction with the statistical theory calculation results performed using TALYS code show that the better agreement is attained in the case of optical potential with the back-shifted Fermi gas level density and Gogny γ-ray strength function parameters.

Acknowledgements. *The paper is a part of the research done within the project 8.2.2.0/20/I/006 LU and VPP-IZM-CERN-2022/1-0001. Institute of Solid State Physics, University of Latvia as the Center of Excellence has received funding from the European Union Horizon 2020 Framework Programme H2020-WIDESPREAD-01-2016-2017-TeamingPhase2 under grant agreement No.739508, project CAMART2.*

References.

1. M. Arnould, S. Goriely, "The p-process of stellar nucleosynthesis: astrophysics and nuclear physics status", *Physics Reports*, **384**(1–2), 1-84, 2003. https://doi.org/10.1016/S0370-1573(03)00242-4
2. L. Funke, H. Graber, K.-H. Kaun, H. Sodan, G. Geske, J. Frána, "Der Zerfall von ^{162}Tb und ^{163}Tb", *Nuclear Physics*, **84**(2), 424-442, 1966. https://doi.org/10.1016/0029-5582(66)90381-6
3. N. Kaffrell, G. Herrmann, *"Der Zerfall des ^{163}Tb"*, *Z. Physik*, **245**, 451–470 (1971). https://doi.org/10.1007/BF01395284
4. C.W. Reich, B. Singh, "Evaluated Nuclear Data File (ENDF)", **111**, 1211, 2010. Retrieved from: https://www-nds.iaea.org
5. O. S. Deiev, I. S. Timchenko, S. N. Olejnik, S. M. Potin, V. A. Kushnir, V. V. Mytrochenko, S. A. Perezhogin, V. A. Bocharov, "Photonuclear reactions ^{nat}Ni(γ,xn)^{57}Ni and ^{nat}Ni(γ,xn)^{56}Ni in the energy range $E_{\gamma max}$ = 35–94 MeV", *Nuclear Physics A*, **1028**, 122542, 2022. https://doi.org/10.1016/j.nuclphysa.2022.122542
6. H. Naik et al., "Photo-neutron cross-section of ^{nat}Gd in the bremsstrahlung end-point energies of 12–16 MeV and 60–70 MeV", *Eur. Phys. J. A*, **58**, 92, 2022.

https://doi.org/10.1140/epja/s10050-022-00736-4

7. T. Bengtsson, I. Ragnarsson, "Rotational bands and particle-hole excitations at very high spin", *Nuclear Physics A*, **436**(1), 14-82, 1985. https://doi.org/10.1016/0375-9474(85)90541-X
8. I. Ragnarsson, A. Sobiczewski, R. K. Sheline, S. E. Larsson, B. Nerlo-Pomorska, "Comparison of potential-energy surfaces and moments of inertia with experimental spectroscopic trends for non-spherical Z = 50–82 nuclei", *Nuclear Physics A*, **233**, 329-356, 1974. https://doi.org/10.1016/0375-9474(74)90460-6
9. A.J. Koning, D. Rochman, J.-Ch. Sublet, N. Dzysiuk, M. Fleming, S. van der Marck, "TENDL: Complete Nuclear Data Library for Innovative Nuclear Science and Technology", *Nuclear Data Sheets*, **155**, 1- 55, 2019. https://doi.org/10.1016/j.nds.2019.01.002
10. A. Gilbert, A. G. W. Cameron, "A composite nuclear-level density formula with shell corrections", *Canadian Journal of Physics*, **43**, 1446-1496, 1965. https://doi.org/10.1139/p65-139
11. W. Dilg, W. Schantl, H. Vonach, M. Uhl, "Level density parameters for the back-shifted fermi gas model in the mass range 40 < A < 250", *Nuclear Physics A*, **217**(2), 269-298, 1973. https://doi.org/10.1016/0375-9474(73)90196-6
12. E. Khan et al., "Photodisintegration of ultra-high-energy cosmic rays revisited", *Astroparticle Physics*, **23**(2), 191–201, 2005. https://doi.org/10.1016/j.astropartphys.2004.12.007
13. R. Capote et al., "RIPL – Reference Input Parameter Library for Calculation of Nuclear Reactions and Nuclear Data Evaluations", *Nuclear Data Sheets*, **110**(12), 3107-3214 2009. https://doi.org/10.1016/j.nds.2009.10.004
14. S. Goriely, "Radiative neutron captures by neutron-rich nuclei and the r-process nucleosynthesis", *Physics Letters B*, **436**(1-2), 10-18, 1998. https://doi.org/10.1016/S0370-2693(98)00907-1
15. S Goriely, E Khan, M Samyn, "Microscopic HFB + QRPA predictions of dipole strength for astrophysics applications", *Nuclear Physics A*, **739**(3–4), 331-352, 2004. https://doi.org/10.1016/j.nuclphysa.2004.04.105